

Preparation and Structural Evaluation of Epithelial Cell Monolayers in a Physiologically Sized Microfluidic Culture Device

Eshan B. Damle¹, Eiichiro Yamaguchi¹, Joshua E. Yao¹, Donald P. Gaver III¹

¹ Department of Biomedical Engineering, School of Science and Engineering, Tulane University

Corresponding Author

Eshan B. Damle

edamle@tulane.edu

Citation

Damle, E.B., Yamaguchi, E., Yao, J.E., Gaver III, D.P. Preparation and Structural Evaluation of Epithelial Cell Monolayers in a Physiologically Sized Microfluidic Culture Device. *J. Vis. Exp.* (185), e64148, doi:10.3791/64148 (2022).

Date Published

July 1, 2022

DOI

10.3791/64148

URL

jove.com/video/64148

Abstract

In vitro microfluidic experimentation holds great potential to reveal many insights into the microphysiological phenomena occurring in conditions such as acute respiratory distress syndrome (ARDS) and ventilator-induced lung injury (VILI). However, studies in microfluidic channels with dimensions physiologically relevant to the terminal bronchioles of the human lung currently face several challenges, especially due to difficulties in establishing appropriate cell culture conditions, including media flow rates, within a given culture environment. The presented protocol describes an image-based approach to evaluate the structure of NCI-H441 human lung epithelial cells cultured in an oxygen-impermeable microfluidic channel with dimensions physiologically relevant to the terminal bronchioles of the human lung. Using phalloidin-based filamentous-actin staining, the cytoskeletal structures of the cells are revealed by confocal laser scanning microscopy, allowing for the visualization of individual as well as layered cells. Subsequent quantification determines whether the cell culture conditions being employed are producing uniform monolayers suitable for further experimentation. The protocol describes cell culture and layer evaluation methods in microfluidic channels and traditional fixed-well environments. This includes channel construction, cell culture and requisite conditions, fixation, permeabilization and staining, confocal microscopic imaging, image processing, and data analysis.

Introduction

Acute respiratory distress syndrome (ARDS) is an acute condition arising from insult to and propagation of injury in the lung parenchyma, resulting in pulmonary edema of the alveoli, inadequate gas exchange, and subsequent hypoxemia¹. This initiates a cycle of pro-inflammatory

cytokine release, neutrophil recruitment, toxic mediator release, and tissue damage, which itself incurs a further inflammatory response². Additionally, pulmonary surfactant, which stabilizes the airways and prevents damage caused by repetitive recruitment/derecruitment (R/D), may be

inactivated or otherwise rendered dysfunctional by the chemical processes occurring during ARDS, resulting in further stress and injury to the surrounding parenchyma³. If sufficient damage is sustained, mechanical ventilation may be necessary to ensure adequate systemic oxygenation⁴. However, mechanical ventilation imposes its own challenges and traumas, including the possibility of ventilator-induced lung injury (VILI), characterized as injury to the lung parenchyma caused by the mechanical stresses imposed during overinflation (volutrauma) and/or the R/D of the air-liquid interface in the fluid-occluded airway (atelectrauma)⁵. The pressure gradient experienced by epithelial cells exposed to an air-liquid interface (as in a fluid-occluded bronchiole) in the atelectrauma model can result in a permeability-originated obstructive response (POOR), leading to a POOR-get-POORer virtuous cycle of injury^{6,7,8}.

In vitro experimentation can provide micro-scale insights into these phenomena, but current studies in microfluidic channel environments with physiologically relevant dimensions face several challenges⁹. For one, optimizing cell culture conditions poses a significant barrier to entry for cell culture research in microfluidic environments, as there exists a narrow intersection within which media flow parameters, culture duration, and other culture conditions permit optimal cell layer formation. This includes the diffusion limitations imposed by the oxygen-impermeable nature of the microfluidic culture channel enclosure. This necessitates careful consideration of media flow parameters, as low flow rates can deprive cells of oxygen, especially those farthest from the inlet; on the other hand, high flow rates can push cells out of the culture channel or result in improper or uneven layer development. Diffusion limitations may be addressed by using oxygen-permeable materials such as polydimethylsiloxane (PDMS) in an air-liquid interface (ALI)

culture apparatus; however, many conventional microfluidic culture channels, such as those of the electric cell-substrate impedance sensing (ECIS) system, are inherently oxygen-impermeable, given the nature of the manufactured enclosure¹⁰. This protocol aims to provide a technique for analyzing cell layers cultured in an oxygen-impermeable enclosure.

When comparing the viability of culture conditions, observations of specific layer characteristics, such as the presence of a monolayer, surface topology, confluence, and layer-thickness uniformity, are necessary to determine whether the cell layer produced by a particular set of culture conditions meets the desired specifications and are indeed relevant to the experimental design. A limited evaluation may be performed by methods such as ECIS, which utilizes measurements of electric potential (voltage) created by resistance to high-frequency alternating current (AC) (impedance) imposed by electrically-insulating membranes of cells cultured on gold electrodes within the flow array. By modulating the frequency of AC applied to cells, specific frequency-dependent cellular properties of the cells and cell layers such as surface adherence strength, tight-junction formation, and cell proliferation or confluence may be targeted and examined¹¹. However, these indirect forms of measurements are somewhat difficult to interpret at the onset of an experiment, and may not quantify all relevant aspects of the cell layer. Simply observing the cell layer under a phase-contrast microscope may reveal the nature of certain qualities such as confluence; however, many relevant characteristics such as the presence of a monolayer and layer-thickness uniformity require a three-dimensional (3D) evaluation that is not possible with brightfield, phase-contrast, or fluorescent microscopic imaging¹².

The objective of this study was to develop a filamentous-actin staining technique to allow for imaging-based verification of a monolayer and the evaluation of cell layer uniformity using confocal laser scanning microscopy (CLSM). Filamentous-actin (F-actin) was deemed an appropriate target for the fluorophore conjugate, due in part to the way that F-actin tightly follows the cell membrane, allowing for a visual approximation of the entire cell volume¹³. Another important benefit of targeting F-actin is the manner in which staining of F-actin visually elucidates cytoskeletal disruptions or alterations imposed by the stresses and strains experienced by the cells. Crosslinking fixation with methanol-free formaldehyde was used to preserve the morphology of the cells and the cell layer, as dehydrating fixatives such as methanol tend to flatten cells, grossly distorting the cell layer and altering its properties^{14,15}.

To determine the ability of the layer evaluation technique to mitigate these challenges, cells were cultured in traditional eight-well culture chambers as well as in microfluidic channels to evaluate the differences, if any, in the cell layers that were produced. For fixed culture wells, eight-well chambered coverglass units were used. For microfluidic culture, flow arrays (channel length 50 mm, width 5 mm, depth 0.6 mm) were optimized to culture immortalized human lung epithelial (NCI-H441) cells in an environment with dimensions physiologically relevant to the terminal bronchioles present in the respiratory zone of the human lung¹⁶. While this protocol was developed with the culture environment of ECIS flow arrays in mind, it may apply to any oxygen-impermeable dynamic-culture environment for which evaluation of cultured cell layer characteristics or culture conditions is necessary.

Protocol

The NCI-H441 human epithelial lung cell line was used for the present study (see **Table of Materials**).

1. Cell culture in the microfluidic channel

1. Fabricate the microfluidic channel and perform the pre-treatment following the steps below.
 1. Obtain a single-channel flow array (see **Table of Materials**) and separate the upper portion from the polycarbonate base plate.
 2. Obtain a #1.5 rectangular coverglass (thickness 0.17 mm) with dimensions of 60 mm x 22 mm. Clean surfaces of the coverglass in an ultrasonic bath and treat one side with a 0.1 mg/mL solution of Poly-D-Lysine at room temperature for 5 min before drying at 60 °C for 30 min.
 3. Affix a 0.13 mm thick double-sided adhesive (see **Table of Materials**), laser-cut to accommodate the dimensions of the flow array top and the flow channel (50 mm length, 5 mm width), to the flow array top, taking care to precisely align the channel cut-outs¹⁷.
 4. Affix a 0.1 mm thick mylar spacer (see **Table of Materials**), laser-cut to accommodate the dimensions of the flow array top and the flow channel, to the adhesive strip, taking care to precisely align the channel cut-outs.
 5. Repeat steps 1.1.3 and 1.1.4 until desired channel height is achieved (for example, for a channel height of 0.6 mm, use two spacers and three adhesive strips).

6. Affix a rectangular coverglass to the bottom-most adhesive strip with the Poly-D-Lysine-treated side facing the adhesive. After assembly is complete, as indicated in **Figure 1**, apply firm and equal pressure to the top and bottom of construction and hold for 1 min.

NOTE: Construction of the channel enclosure, including coverglass, adhesives, spacers, and flow array top, is now complete.

7. Rinse the channel with de-ionized water using a syringe, simultaneously checking for leaks.
8. Sterilize channel enclosure in an ultraviolet (UV) sterilizer for 30 min¹⁸.
9. Using sterile technique, treat the channel with 2.0 µg/mL human fibronectin (see **Table of Materials**) in phosphate buffered saline (PBS) and incubate for at least 30 min at 37 °C¹⁹.

2. Perform cell culture in the microfluidic channel following the steps below.

1. In a sterile laminar flow hood, use a micropipette to transfer an even suspension of NCI-H441 cells in RPMI 1640 medium with 10% fetal bovine serum (FBS) (see **Table of Materials**) to seed two microfluidic channels, each with cells at a surface density of 150,000 cells/cm².

1. For 50 mm x 5 mm x 0.6 mm channels, use 0.25 mL of a 2.5×10^6 cells/mL suspension to fill each channel, as well as a portion of the ports. Verify that cells have been distributed evenly within the channels using a brightfield microscope.

2. Culture the two channels for 24 h and 48 h respectively at 37 °C with 5% CO₂ using a programmable syringe pump (see **Table of Materials**), drawing spent media out from the channel and fresh media into the channel from a sterile media reservoir attached to channel inlet comprised of a cut-open 20 mL syringe covered with paraffin film.

1. After a 10 min waiting period following cell seeding, introduce and pump fresh media from the reservoir through the channel at a variable flow rate beginning at 0.2 µL/min and ramping up to 10 µL/min for 4 h, maintaining at that rate thereafter²⁰.

NOTE: This variable flow rate provides culture conditions that allow cells to (1) gravitationally settle to the culture surface, (2) adhere to the culture surface, and (3) form a confluent monolayer.

3. Perform cell fixation inside the microfluidic channels using formaldehyde solution.

CAUTION: Formaldehyde is toxic and must be handled in an appropriate chemical fume hood²¹.

1. In a chemical fume hood, prepare formaldehyde solutions by using 4% formaldehyde in PBS (methanol-free) (see **Table of Materials**) to create two 4 mL portions, diluting the first to a concentration of 1% formaldehyde and the second to 2% formaldehyde using Dulbecco's phosphate buffered saline (DPBS; with Ca²⁺ and Mg²⁺) as the diluent. Transfer formaldehyde solutions to separate 5 mL syringes and label accordingly. Draw up 20 mL of DPBS into a separate 20 mL syringe.

2. Remove microfluidic channels from the culture apparatus and place them into the chemical fume hood.
3. Assemble the fixation and staining apparatus.
 1. Attach a 10 cm segment of transfer tubing to the side port of a three-way stopcock *via* a male Luer lock to hose barb adapter (see **Table of Materials**), then connect the stopcock to the inlet port of the flow array.
 2. Next, attach another 10 cm segment of transfer tubing to the outlet port of the flow array using the same type of hose barb adapter.
 3. Finally, secure the free ends of both transfer tubes in a chemical and biohazard-appropriate waste container, such as a labeled empty 50 mL conical centrifuge tube.
4. Turn the stopcock to block off the flow array inlet port and flush the waste line with DPBS. Then, turn the stopcock to block off the waste line and slowly wash cells with 2 mL of DPBS. Repeat the flushing step using the new solution every time. A new solution (or concentration of solution) is introduced to the channel.
5. Slowly push 2 mL of 1% fixative solution through the channel and then allow to sit for 5 min²².
6. Slowly push 2 mL of 2% fixative solution through the channel and then allow to sit for 15 min.
7. Wash cells by slowly introducing 2 mL of fresh DPBS to the channel in three separate instances (5 min each).
8. Complete steps 1.3.3-1.3.7 for both microfluidic channels in parallel.
4. Stain, permeabilize, and add mounting media to the cells in the microfluidic channel.
 1. Prepare 0.1% saponin solution by adding 1 mg of saponin (see **Table of Materials**) per mL of DPBS to produce 4 mL of solution and gently vortex to mix²³. Draw up 8 mL of DPBS into a 20 mL syringe.
 2. Add an F-actin-staining phalloidin reagent and a nucleus-staining Hoechst reagent (see **Table of Materials**) to the 0.1% saponin solution, at two drops (0.1 mL) of each reagent per mL of saponin solution. Keep prepared staining/permeabilizing solution away from light by covering with aluminum foil²⁴.
 3. Flush the line with a small amount of staining/permeabilizing solution (as described in step 1.3.4), then introduce 2 mL of the solution to the microfluidic channel and cover the channel with aluminum foil before allowing it to sit at room temperature for 30 min.
 4. Flush out the staining/permeabilizing solution twice with 2 mL of DPBS for 5 mins per flush.
 5. For better image quality, add a suitable mounting media (with an index of refraction closely matching the microscope objective oil and cover glass, see **Table of Materials**) into the channel.
 1. Using a micropipette, introduce a minimal amount of a soft-set antifade mountant to each port of the microfluidic channel, ensuring that the bottom surface is completely covered and no bubbles are trapped within the desired imaging area²⁵. Seal the ends of the channel

and verify cell layer integrity by observing under a brightfield microscope.

6. Complete steps 1.4.3-1.4.5 for both microfluidic channels in parallel.

NOTE: Image cells as soon as possible after staining for maximum image quality. If photobleaching occurs or long-term storage is desired, other mounting media with antifade or sample-preserving properties may be used. Note that hard-curing mounting media will distort the 3D structure of the cells and, by extension, the cell layer; for this reason, soft-setting mounting media is preferable²⁶.

5. Image cells in the microfluidic channel following the steps below.

1. Adjust the confocal microscope (see **Table of Materials**) settings, including laser power, gain, offset, and scan parameters such as scan speed, scan area, scan format, resolution, and pinhole diameter²⁷.
2. Test imaging location by taking reference scans as well as Z-stacks until desired image parameters and conditions have been met. Dial-in parameters at sequentially higher-magnification objectives until the 40x oil-immersion objective has been reached and optimized²⁸.
3. Using the flow array base plate as a reference, construct Z-stacks at five locations, at the would-be location of the first electrode on the inlet

side, halfway between the center and the previous location, the center, halfway between the center and the location of the last electrode (on the outlet side), and at the last electrode, as indicated in **Figure 2**.

6. Perform image processing and data analysis.
 1. Export XZ and YZ cross-sections using the confocal microscope software package (see **Table of Materials**).
 2. Using an image-processing software (see **Table of Materials**) with edge-detection capabilities (thresholding value 15.0), measure the total image area in pixels by using the **Magic Wand tool** outside of the image, then the area excluding the total cross-sectional area of the cell layer in pixels by using the **Magic Wand tool** in the portion of the image exterior to the cell layer²⁹.
 3. Using data-processing software (see **Table of Materials**), subtract the exterior area pixel value from the total area pixel value to find the cross-sectional area pixel value.
 4. Convert cross-sectional area pixel values to μm^2 values by multiplying pixel values by the square of the $\mu\text{m}/\text{pixel}$ value, as indicated in the microscope software for the particular image (0.31 $\mu\text{m}/\text{pixel}$ for Z-stacks taken in 1024p resolution with no zoom on a 40x oil-immersion lens).
 5. Calculate means and standard deviations of data and graph results.

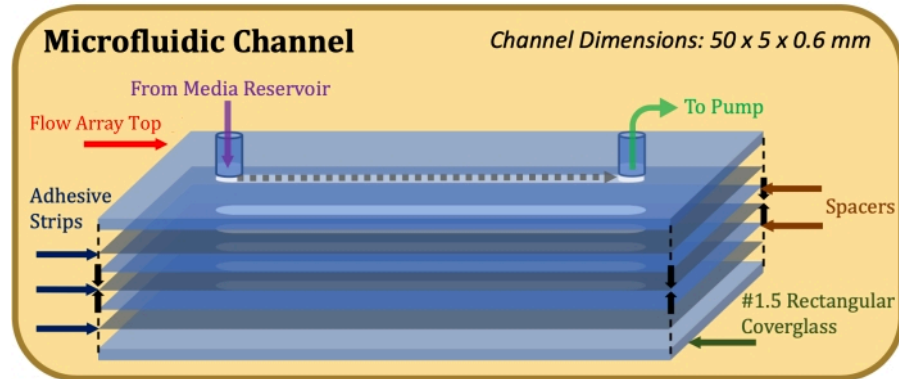


Figure 1: Exploded-view schematic of the microfluidic channel construction. The top element is the top portion of the flow array, thin grey elements are adhesive strips, thin blue elements are mylar spacers, and the bottom element is the rectangular coverglass. [Please click here to view a larger version of this figure.](#)

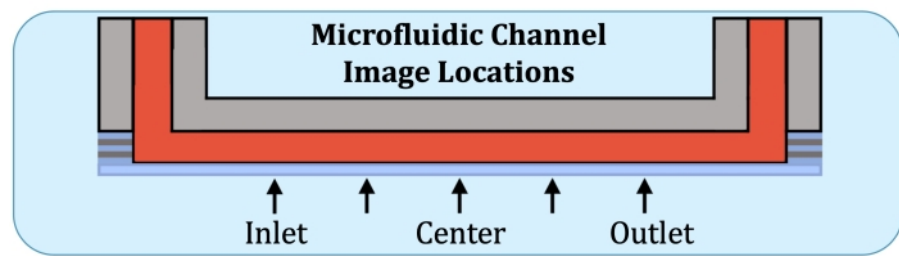


Figure 2: Five imaging locations along the consistently layer-producing region of the microfluidic culture channel. Imaging locations are as follows: inlet-side, near where the first electrode would be on the intact flow array; halfway between inlet-side location and the center of the channel; center of the channel; halfway between the center and the outlet-side location, and outlet-side, near where the last electrode would be on the intact flow array. [Please click here to view a larger version of this figure.](#)

2. Cell culture in the eight-well chambered coverglass

1. Perform pre-treatment of the eight-well chambered coverglass.

1. Obtain a sterile eight-well chambered coverglass manufactured with a #1.5 coverglass and cell adherence-increasing surface treatment (**Figure 3**, see **Table of Materials**).

2. Using sterile technique, treat the surface of culture wells with 2.0 μ g/mL human fibronectin in PBS and incubate for at least 30 min at 37 °C¹⁹.
2. Perform cell culture in the chambered coverglass following the steps below.
 1. In a sterile laminar flow hood, transfer 0.5 mL portions of solutions of NCI-H441 cells evenly suspended in RPMI 1640 medium with 10% FBS at volumetric densities of 81,000, 162,000, and 324,000 cells/mL to seed the culture wells at surface densities of 45,000, 90,000, and 180,000 cells/cm², respectively. Verify that cells have been evenly distributed within the wells using a brightfield microscope.
 2. Culture cells for 24 h, 48 h, and 96 h at 37 °C with 5% CO₂, replacing media daily.
 3. Perform formaldehyde fixation in the eight-well chambered coverglass.

CAUTION: Formaldehyde is toxic and must be handled in an appropriate chemical fume hood²¹.

 1. In a chemical fume hood, prepare formaldehyde solutions by making two portions of 4% formaldehyde in PBS (methanol-free), diluting the first to a concentration of 1% formaldehyde and the other to 2% formaldehyde using Dulbecco's phosphate buffered saline (DPBS; with Ca²⁺ and Mg²⁺) as the diluent.
 2. Remove the eight-well culture chambered coverglass from the incubator and place it into the chemical fume hood.
 3. Gently wash cells with 0.5 mL of DPBS using a micropipette by slowly introducing liquid along the upper portion of the corner of each well.
 4. Remove existing liquid in each well by slowly extracting it from the corner of the wells using a micropipette. Using the liquid-introduction method (step 2.3.3), introduce 0.5 mL of 1% fixative solution into each well and allow it to sit for 5 min²².
 5. Remove existing liquid in each well using the liquid-extraction method mentioned in step 2.3.4. Using the liquid-introduction method mentioned in step 2.3.3, introduce 0.5 mL of 2% fixative solution into each well and allow it to sit for 15 min.
 6. Using the liquid introduction and extraction methods (steps 2.3.3 and 2.3.4), wash cells by introducing and removing 0.5 mL of fresh DPBS in each well in three separate instances for 5 min each.
 4. Perform staining, permeabilization, and mounting media addition in the eight-well chambered coverglass.
 1. Prepare 0.1% saponin solution by adding 1 mg of saponin per mL of DPBS and gently vortex to mix²³.
 2. To the 0.1% saponin solution, add two drops (0.1 mL) each of an F-actin-staining phalloidin reagent and a nucleus-staining Hoechst reagent per mL of saponin solution. Keep the prepared solution away from light by covering with aluminum foil²⁴.
 3. Introduce 0.2 mL of staining/permeabilizing solution to each well and cover the chambered coverglass with aluminum foil before allowing it to sit at room temperature for 30 min.
 4. Flush out staining/permeabilizing solution twice with 0.5 mL of DPBS.

5. For better image quality, add a suitable mounting media (with an index of refraction closely matching the microscope objective oil and cover glass) into the wells.
 1. Using a micropipette, introduce a minimal amount of a soft-set antifade mountant to each well, ensuring that the bottom surface is completely covered and no bubbles are trapped within the desired imaging area²⁵. Verify cell layer integrity by observing under a brightfield microscope.

NOTE: Image cells as soon as possible after staining for maximum image quality. If photobleaching occurs or long-term storage is desired, other mounting media with antifade or sample-preserving properties may be used. Note that hard-curing mounting media will distort the 3D structure of the cells and, by extension, the cell layer, so soft-setting mounting media is preferable²⁶.

- 5. Perform imaging in the eight-well chambered coverglass.
 1. Adjust the confocal microscope settings, including laser power, gain, offset, and scan parameters such as scan speed, scan area, scan format, resolution, and pinhole diameter²⁷.
 2. Test imaging location by taking reference scans as well as Z-stacks until desired image parameters and conditions have been met. Dial-in parameters at sequentially higher-magnification objectives until the 40x oil-immersion objective has been reached and optimized²⁸.
 3. Construct Z-stacks of three random locations in each seeding density/culture duration match-up.
 6. Perform image processing and data analysis.
 1. Export XZ and YZ cross sections using the confocal microscope software package.
 2. Using an image-processing software with edge-detection capabilities (thresholding value 15.0), measure the total image area in pixels by using the **Magic Wand tool** outside of the image, then the area excluding the total cross-sectional area of the cell layer in pixels by using the **Magic Wand tool** in the portion of the image exterior to the cell layer²⁹.
 3. Using a data-processing software, subtract the exterior area pixel value from the total area pixel value to find the cross-sectional area pixel value.
 4. Convert cross-sectional area pixel values to μm^2 values by multiplying pixel values by the square of the $\mu\text{m}/\text{pixel}$ value as indicated in the microscope software for the particular image (0.31 $\mu\text{m}/\text{pixel}$ for Z-stacks taken in 1024p resolution with no zoom on a 40x oil-immersion lens).
 5. Calculate means and standard deviations and graph results.

8-Well Chambered Coverglass

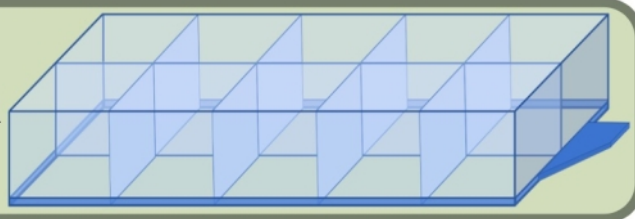


Figure 3: Diagram of the eight-well chambered coverglass used for the fixed-well culture, staining, and imaging experiment comparing the effects of initial cell seeding density and culture duration on the formation of cell layers.

[Please click here to view a larger version of this figure.](#)

Representative Results

The presented method allows for the visualization of epithelial cell layers cultured in microfluidic culture channels and uses a demonstration in traditional fixed-well cell culture environments as validation. Images acquired will exist on a spectrum of quality, signal intensity, and cellular target specificity. Successful images will demonstrate high contrast, allowing for image analysis and quantification of data for subsequent statistical evaluation. Unsuccessful images will be dim, fuzzy, blurry, or otherwise unusable for subjective or quantitative evaluation. Some images may be suitable for subjective layer characteristic determination while still being of insufficient quality for quantitative analysis. Thus, the degree and care to which the protocol is followed will directly impact the suitability of a given image to serve as a data source for statistical analysis.

Figure 4 represents the successful use of the technique in the context of a microfluidic dynamic-culture environment and shows image acquisition at the inlet and outlet of two microfluidic devices. **Figure 4A,B** provides examples of layers cultured for 24 h, and **Figure 4C,D** presents examples

of layers cultured for 48 h. **Figure 5** illustrates the associated data collected from the microfluidic channel experiment, incorporating three samples from each of the five microfluidic channel imaging locations indicated in **Figure 2** from each culture duration. Error bars signify standard deviations.

Figure 6 depicts a 2D image of the XY plane in the center of the microfluidic channel, and **Figure 7** depicts a 3D view of the same location with depth color-coding. **Figure 8** represents successful image acquisition within a density-duration experiment analyzing the effects of initial cell seeding density and culture duration on NCI-H441 cell layer formation in the eight-well chambered coverglass environment. **Figure 8A-C** indicates culture durations of 24 h, 48 h, and 96 h, respectively. **Figure 8X-Z** indicates initial cell seeding densities of 180,000, 90,000, and 45,000 cells/cm², respectively. **Figure 9** presents quantitative data collected from the eight-well chambered coverglass experiment, including samples from three locations in each density-duration match-up. Error bars represent standard deviations and *p*-value tests were performed to determine statistically significant differences between apparently close values.

These two representative experiments within the dynamic microfluidic and static eight-well environments are distinct use-case examples that demonstrate how the technique may

contextualize experimental findings by visually confirming the presence or absence of physiologically relevant monolayers.

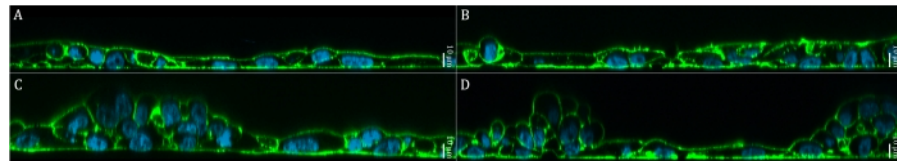


Figure 4: NCI-H441 cell layers cultured in the microfluidic channel for 24 and 48 h, imaged at the inlet-side and outlet-side locations as depicted in Figure 2. (A) 24 h, inlet-side. (B) 24 h, outlet-side. (C) 48 h, inlet-side. (D) 48 h, outlet-side. Blue represents the nuclei staining and green represents the staining of filamentous-actin. [Please click here to view a larger version of this figure.](#)

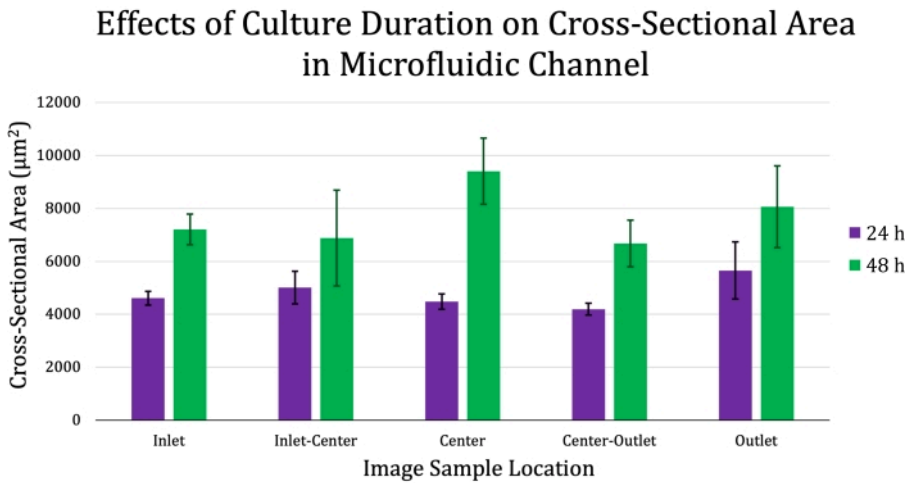


Figure 5: Graphical representation of the data collected during the 24-48 h microfluidic channel imaging experiment. This includes six cross-sectional area samples from each of five locations along the relevant length of the microfluidic channel (as depicted in Figure 2). Error bars represent standard deviations. [Please click here to view a larger version of this figure.](#)

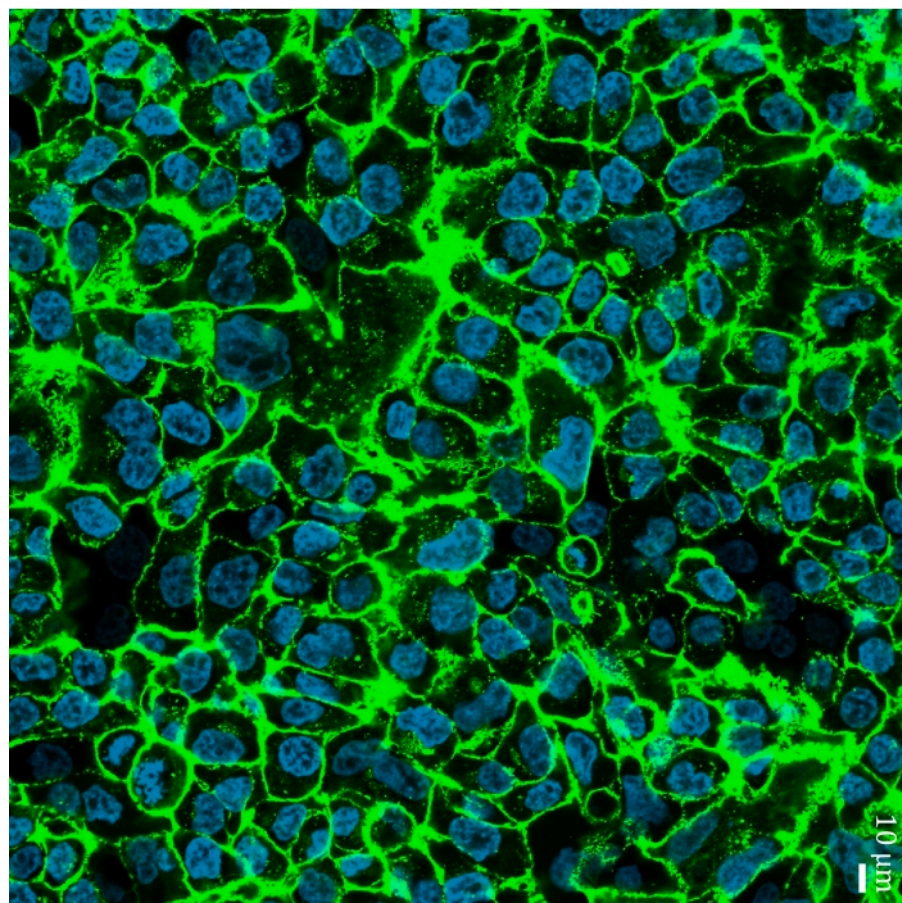


Figure 6: 2D image taken in the XY plane in a central location within the microfluidic channel. Blue represents the nuclei staining and green represents the staining of filamentous-actin. [Please click here to view a larger version of this figure.](#)

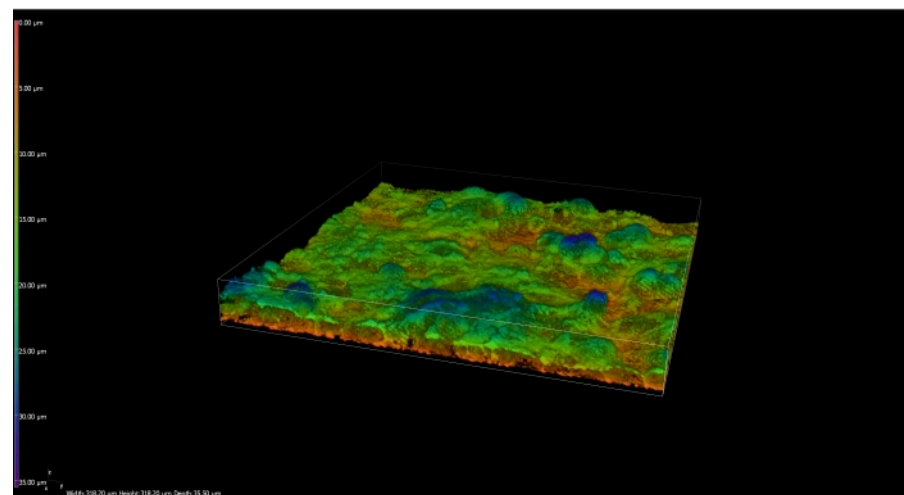


Figure 7: 3D model of the same microfluidic channel location as Figure 6. The color-coding depicts depth data. [Please click here to view a larger version of this figure.](#)

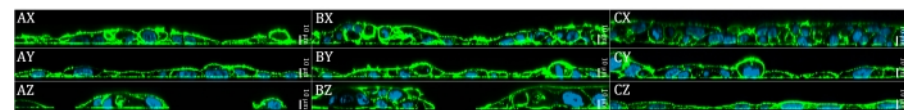


Figure 8: NCI-H441 cell layers cultured in the eight-well chambered coverglass. For 24 h (**A**), 48 h (**B**), and 96 h (**C**) at initial seeding densities of 180,000 (**X**), 90,000 (**Y**), and 45,000 (**Z**) cells/cm². Blue represents the nuclei staining and green represents the staining of filamentous-actin. [Please click here to view a larger version of this figure.](#)

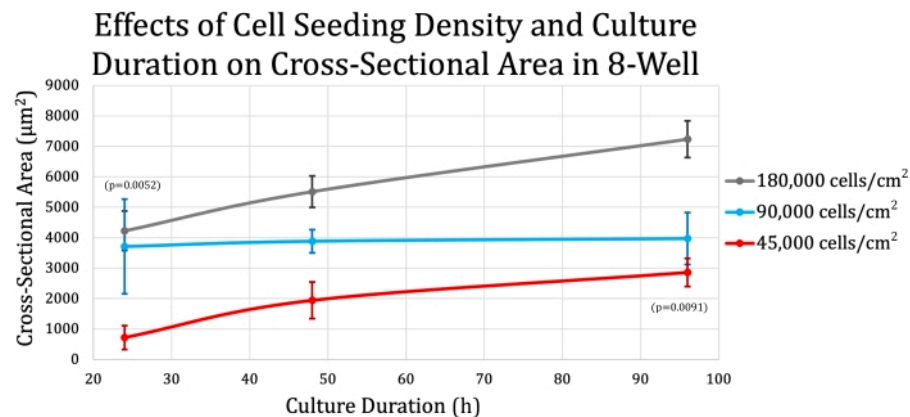


Figure 9: Graphical representation of the data collected during the density-duration eight-well culture experiment.

This includes six cross-sectional area samples from each density-duration match-up. Error bars represent standard deviations. [Please click here to view a larger version of this figure.](#)

Discussion

The presented protocol describes the culture, crosslinking fixation, staining, permeabilization, and confocal microscopic visualization of NCI-H441 human lung epithelial cells in the dynamic environment of a single-channel microfluidic flow array, as well as in the static environment of a traditional eight-well chambered coverglass. With any microfluidic cell culture protocol, the flow conditions of the cell culture media are of paramount importance, as the high-rate flow has the potential to wash away the cells or interfere with the normal assembly of the cell monolayer. Meanwhile, low-rate flow has the potential to "starve" or "suffocate" (insufficient nutrient and oxygen availability, respectively) the cell layer due to the diffusion limitations imposed by the impermeable nature of the microfluidic channel as well as the flow characteristics³⁰. By beginning with a 10 min waiting period (during which cells remain suspended in the same media that originally filled the channel), then advancing to a flow rate of 0.2 μ L/min, before finally ramping up to 10 μ L/min over the course of 4

h, these competing needs are balanced to promote both cell adherence and survival.

Another critical step in the protocol is the proper preparation of the microfluidic channel, including construction and pre-treatment. Care must be taken to ensure that the coverglass is mounted properly to the chamber construct to avoid leakage and potential contamination. Proper attachment of the coverglass is also necessary to ensure that the channel height is consistent and accurately reproduced between successive trials using different constructed units. Minor variability may be introduced by the tolerance in thickness of the adhesive strips used as well as the relative compressibility. Minimizing any variability will help with the consistency of experimental results. Proper pre-treatment of the constructed channel is important to ensure that the cells are allowed to adhere to and initiate proliferation on the glass surface. Ultrasonic cleaning of the glass improves Poly-D-Lysine adherence, promoting adherence to fibronectin. Adding fibronectin, a glycoprotein naturally synthesized and secreted by human epithelial cells,

further promotes the adherence of the NCI-H441 cells to the coverglass surface, allowing for normal cell monolayer development³¹.

Further, one of the most important aspects of this protocol is the imaging location. Despite carefully controlled preparation, due to the columnar volume available in the regions of the two channel openings, more cells will be present on the coverglass surface in the area directly underneath as well as adjacent to these openings, even when adhering to proper cell culture techniques. For this reason, regions near the openings should not be considered as part of the "normal" cultured cell layer, as there will be significant multilayering/cell-stacking occurring there. Instead, the central region of the microfluidic channel is an appropriate area to image, as this location is undisturbed by the error imposed by channel height variation near the openings. The electrode locations on the flow array can be used to guide imaging locations, and as a rule of thumb, all scans intended to capture layers truly representative of the microfluidic channel conditions should be taken at analogous locations within the bounds of the two farthest-apart electrodes on the flow array. Additionally, in the protocol described, the 40x magnification objective is specified for use; however, this may be modified to suit the user's needs. 40x magnification was chosen as the optimal magnification because of its ability to offer high-resolution, high-magnification imaging while still retaining a sufficient number of cells to serve as a statistically valid sample.

One modification that can be made to the microfluidic channel includes altering the channel height, which can be achieved by varying the number of spacers and adhesives used to construct the microfluidic channel. Alteration of the channel height will likely necessitate adjusting the flow parameters to ensure that the shear stress does not remove cells during the

feeding. As such, any variation in channel height will impact the ideal initial rate, rate of ramp-up, and final rate of media flow. The described protocol in this article may serve as a means by which suitable flow rates may be experimentally derived, in conjunction with indirect methods such as ECIS. Additionally, flow rates may be modified to suit the needs of different cell lines, which may require adaptation to establish optimal conditions. Another modification that may be made, with some additions to the steps in this protocol, is to expand the use-case of the described technique beyond the relative comparison of the cross-sectional area of cell layers. With appropriate calibration using microspheres or microbeads of known dimensions, accurate volumetric, topologic, and absolute cross-sectional area measurements may be taken. Calibration using a reference object is necessary in this instance due to the confocal microscope's limited Z-resolution and the potential for over- or under-sampling in the Z-dimension due to the manual control over Z-stack step size that confocal scanning systems offer³².

One limitation of this protocol is the lack of true volumetric measurement due to the lack of vertical calibration steps. The calibration mentioned above and the verification technique utilizing fluorescent microbeads of known dimensions may be used for true-to-life scaling. Additionally, the present protocol involves the use of pre-prepared, ready-to-use stains. Immunofluorescent staining using primary and secondary antibodies often requires a multi-day protocol that is more involved than the one this article discusses. However, it is likely possible to utilize immunofluorescent staining in this manner, though some experimentation may be necessary to optimize the workflow. Given the additional steps involved in immunofluorescent staining protocols, care must be taken to avoid shearing of the cultured cell layer during the numerous wash steps, as this may alter the properties of the cell layer

ultimately evaluated and therefore invalidate any conclusions that would follow. Further developments of this technique may include automation of the image and data analyses, including region-of-interest (ROI) detection and quantification for the cross-sectional area determination. Additionally, expanding this technique to include different intra- and extra-cellular target structures (perhaps staining for targets such as tight-junction proteins) may broaden the use-case of this method to 3D co-localization within microfluidic cell culture devices.

To produce the most physiologically representative cell layers, lung epithelial cells must be cultured in microfluidic channels with an air-liquid interface (ALI) at the culture surface, which is typically accomplished using polydimethylsiloxane (PDMS), a flexible material made permeable by the introduction of μm -scale pores. ALI culture conditions allow for the formation of cell layers that most closely resemble the physiological features of the *in vivo* lung epithelium³³. While technically possible, using ECIS in an ALI culture environment with a PDMS culture surface in a dynamic microfluidic environment is impractical and inaccessible for most researchers, as there are no commercially available apparatuses for such a complex cell culture assembly³⁴. One reason for this difficulty may be the paradoxical need for a permeable culture surface that is still capable of acting as a solid electrode for the purpose of ECIS measurements. As such, there currently exists the need for a method to visually verify the characteristics and physiologic relevance of cell layers cultured in oxygen-impermeable culture environments such as those present in ECIS flow arrays.

This method expands on the traditional method of ensuring proper confluence using two-dimensional microscopy by allowing for 3D visualization, which greatly broadens the number of cell layer characteristics that can be observed,

quantified, and analyzed. Additionally, this permits a subjective determination of the presence of a monolayer, layer uniformity, and other properties deemed relevant for experimental purposes. This protocol is important because it serves as a means for the visual verification and evaluation of cell layers being produced in many oxygen-impermeable environments, such as in ECIS experiments evaluating barrier function properties of epithelial cells exposed to atelectrauma. This also serves as a method that can be used in future work to determine whether a set of dynamic microfluidic culture conditions produces cell layers that are relevant and appropriate for further experimentation.

Disclosures

The authors declare no conflicts of interest.

Acknowledgments

The authors acknowledge Alan Shepardson for designing the cutting pattern for the 3M adhesive and mylar sheet used in microfluidic channel construction and for testing the cell culture media flow rate and syringe pump programming. Funding was supplied by NIH R01 HL0142702, NSF CBET 1706801, and the Newcomb-Tulane College Dean's Grant.

References

1. Matthay, M. A. et al. Acute respiratory distress syndrome. *Nature Reviews Disease Primers*. **5**, 18 (2019).
2. Rawal, G., Yadav, S., Kumar, R. Acute respiratory distress syndrome: An update and Review. *Journal of Translational Internal Medicine*. **6** (2), 74-77 (2018).
3. Bilek, A. M., Dee, K. C., Gaver, D. P. Mechanisms of surface-tension-induced epithelial cell damage in a model of pulmonary airway reopening. *Journal of Applied Physiology*. **94** (2), 770-783 (2003).

4. Modrykamien, A. M., Gupta, P. The acute respiratory distress syndrome. *Baylor University Medical Center Proceedings*. **28** (2), 163-171 (2017).

5. Jacob, A.-M., Gaver, D. P. Atelectrauma disrupts pulmonary epithelial barrier integrity and alters the distribution of tight junction proteins ZO-1 and Claudin 4. *Journal of Applied Physiology*. **113** (9), 1377-1387 (2012).

6. Kay, S. S., Bilek, A. M., Dee, K. C., Gaver, D. P. Pressure gradient, not exposure duration, determines the extent of epithelial cell damage in a model of pulmonary airway reopening. *Journal of Applied Physiology*. **97** (1), 269-276 (2004).

7. Jacob, A. M., Gaver, D. P. An investigation of the influence of cell topography on epithelial mechanical stresses during pulmonary airway reopening. *Physics of Fluids*. **17** (3), 031502 (1994).

8. Gaver, D. P. et al. The POOR get POORer: A hypothesis for the pathogenesis of ventilator-induced lung injury. *American Journal of Respiratory and Critical Care Medicine*. **202** (8), 1081-1087 (2020).

9. Jain, P. et al. Reconstruction of ultra-thin alveolar-capillary basement membrane mimics. *Advanced Biology*. **5** (8), 2000427 (2021).

10. Byrne, M. B., Leslie, M. T., Gaskins, H. R., Kenis, P. J. A. Methods to study the tumor microenvironment under controlled oxygen conditions. *Trends in Biotechnology*. **32** (11), 556-563 (2014).

11. Szulcek, R., Bogaard, H. J., van Nieuw Amerongen, G. P. Electric cell-substrate impedance sensing for the quantification of endothelial proliferation, barrier function, and motility. *Journal of Visualized Experiments*. (85), e51300 (2014).

12. Jaccard, N. et al. Automated method for the rapid and precise estimation of adherent cell culture characteristics from phase contrast microscopy images. *Biotechnology and Bioengineering*. **111** (3), 504-517 (2013).

13. Hagiwara, M. et al. Modest static pressure suppresses columnar epithelial cell growth in association with cell shape and cytoskeletal modifications. *Frontiers in Physiology*. **8**, 00997 (2017).

14. Srinivasan, M., Sedmak, D., Jewell, S. Effect of fixatives and tissue processing on the content and integrity of Nucleic Acids. *The American Journal of Pathology*. **161** (6), 1961-1971 (2002).

15. Zhu, L., Rajendram, M., Huang, K. C. Effects of fixation on bacterial cellular dimensions and integrity. *Iscience*. **24** (4), 102348 (2021).

16. Lust, R. M. *The Pulmonary System. XPharm: The Comprehensive Pharmacology Reference*. 1-6, Elsevier (2007).

17. EpilogueLaser. *FusionSeries: Pro & Edge Laser System Manual and Original Instructions*. Golden, CO: Author. (2022).

18. Chitnis, D. S., Katara, G., Hemvani, N., Chitnis, S., Chitnis, V. Surface disinfection by exposure to germicidal UV light. *Indian Journal of Medical Microbiology*. **26** (3), 241 (2008).

19. Sandell, L., Sakai, D. Mammalian cell culture. *Current Protocols Essential Laboratory Techniques*. **5** (1), 4-3 (2011).

20. New Era Pump Systems. *Multi-Phaser Programmable Syringe Pump: NE-1000 Series User Manual*. Farmingdale, NY: Author. (2014).

21. ThermoFisher Scientific. *Safety Data Sheet: ImageiT Fixative Solution (4% formaldehyde, methanol-free)*. Waltham, MA: Author. (2018).

22. Thavarajah, R., Mudimbaimannar, V. K., Rao, U. K., Ranganathan, K., Elizabeth, J. Chemical and physical basics of routine formaldehyde fixation. *Journal of Oral and Maxillofacial Pathology*. **16** (3), 400-405 (2012).

23. Jamur, M. C., Oliver, C. Permeabilization of cell membranes. *Immunocytochemical Methods and Protocols*. **588**, 63-66 (2009).

24. ThermoFisher Scientific. *ActinGreen 488 ReadyProbes Reagent Protocol*. Waltham, MA: Author. (2022).

25. Author. *Slowfade Glass soft-set Antifade Mountant*. Thermo Fisher Scientific - US. Retrieved February 14, 2022, from <https://www.thermofisher.com/order/catalog/product/S36917-5X2ML?SID=srch-hj-S36917-5X2ML>. (2022).

26. Ravikumar, S., Surekha, R., Thavarajah, R. Mounting media: An overview. *Journal of Dr. NTR University of Health Sciences*. **3** (5), 1-8 (2014).

27. Shihan, M. H., Novo, S. G., Le Marchand, S. J., Wang, Y., Duncan, M. K. A simple method for quantitating confocal fluorescent images. *Biochemistry and Biophysics Reports*. **25**, 100916 (2021).

28. North, A. J. Seeing is believing? A beginners' guide to practical pitfalls in image acquisition. *Journal of Cell Biology*. **172** (1), 9-18 (2006).

29. Ferriera, F., Rasband, W. *ImageJ User Guide*. National Institutes of Health. Bethesda, MD. (2012).

30. Halldorsson, S., Lucumi, E., Gómez-Sjöberg, R., Fleming, R. M. T. Advantages and challenges of microfluidic cell culture in polydimethylsiloxane devices. *Biosensors and Bioelectronics*. **63**, 218-231 (2015).

31. Smith, H. S., Riggs, J. L., Mosesson, M. W. Production of fibronectin by human epithelial cells in culture. *American Association for Cancer Research*. **39** (10), 4138-4144 (1979).

32. Sieck, G. C., Mantilla, C. B., Prakash, Y. S. [17] Volume measurements in confocal microscopy. In *Methods in Enzymology*. **307**, 296-315. Academic Press. (1999).

33. Heijink, I. H. et al. Characterisation of cell adhesion in airway epithelial cell types using electric cell-substrate impedance sensing. *European Respiratory Journal*. **35** (4), 894-903 (2009).

34. Zhang, X., Wang, W., Li, F., Voiculescu, I. Stretchable impedance sensor for mammalian cell proliferation measurements. *Lab on a Chip*. **17** (12), 2054-2066 (2017).